Contribution of the pseudoscalar and vector mesons to the nucleon's g_1 structure function

F. Zamani
Department of Physics, Villanova University, Villanova, Pennsylvania 19085, USA
(Received 31 July 2003; published 21 November 2003)

This is the third part of a series of work that we have done in the context of the meson cloud model. In the first two parts [F. Zamani, Phys. Rev. C **58**, 3641 (1998); F. Zamani and D. Saranchak, Phys. Rev. C **63**, 065202 (2001)] we used pseudoscalar mesons to calculate unpolarized and polarized quark distribution functions along with the nucleon's F_2 and g_1 structure functions. Now we have added the vector mesons to the meson cloud to calculate the polarized quark distribution functions and g_1 structure function. The calculation is performed in the light-cone frame. The dressed nucleon is assumed to be a superposition of the bare nucleon plus virtual light-cone Fock states of baryon-meson pairs. For bare nucleon we consider both the case of diquark-quark clustering and the case where there is no quark clustering inside the nucleon. The initial distributions are evolved. The final results are compared with experimental results and other theoretical predictions.

DOI: 10.1103/PhysRevC.68.055202 PACS number(s): 12.39.Ki, 14.20.Dh, 14.65.Bt, 24.85.+p

I. INTRODUCTION

In 1972 Sullivan pointed out the significance of the pionic structure of the nucleon in high energy processes [1]. Sullivan examined the role of the one-pion exchange in deep inelastic scattering from nucleons. Being the lightest meson, the pion is expected to paly a dominant role in the nucleon structure. However, this does not exclude the contribution of other mesons to the nucleon structure. Therefore, the mesonic structure of the nucleon, or the so-called meson cloud, can have contributions not only from the pion but from other members of the pseudoscalar and vector mesons octets. In recent years there has been an extensive investigation of both unpolarized [3–28] and polarized [2,29–35] nucleon structure using the meson cloud model.

Since late 1980s, there has been a flurry of activities, investigating the spin structure of the nucleon. What started it all were measurements by European Muon Collaboration (EMC), indicating that only a small fraction of the proton spin is carried by the spin of the quarks [36,37]. In the light of the fact that this was in disagreement with quark model prediction, a model which had great success in describing the gross features of the nucleon, the EMC result caused quite a stir in the particle physics community. This resulted in what came to be known as the "proton spin crisis" and resulted in considerable amount of both theoretical and experimental investigation of the nucleon spin. Since then literally hundreds of papers have been published on this subject. On the experimental side, the original experiment by EMC at CERN was followed by Spin Muon Collaboration (SMC) [38–46]. Also, at Stanford Linear Accelerator Center (SLAC) [47–56] and HERMES Collaboration at Deutsches Elektronen-Synchrotron (DESY) [57–60]. Among other things, these experiments have confirmed the original EMC result, the Bjorken sum rule (BSR) [61,62], but show the violation of Ellis-Jaffe sum rule (EJSR) [63], and what appears to be a rather large negative strange quark polarization.

The objective of the theoretical work is to find the contribution of different sources, i.e., quarks, gluons, and orbital motion of the partons, to the spin of the proton. In the late 1980s, Altarelli and Ross [64] and Carlitz, Collins, and Mueller [65] suggested that there is a hard gluonic contribution to the first moment of g_1 structure function of the proton. Others followed up on this suggestion [66–68]. The objective here was to see whether there exists a positive gluon polarization, since this would explain away the rather large negative sea polarization and rather small contribution of the quarks to the spin of the proton. For a period of time there was some apparent conflict between chiral invariant approach and gauge invariant approach to the calculation of the contribution of the gluon to the quark polarization. The reason being that in operator product expansion approach, which is model independent, the hard gluons at twist-2 level make no contribution to the first moment of g_1 structure function This apparent problem has been clarified since the work done in Refs. [67,69] and now the general understanding is that there is a rather significant contribution due to gluon anomaly, which is not unexpected in pQCD regime [70]. Therefore, the observed experimental results are superposition of the quark and gluon polarizations, and therefore, there is no spin crisis. For interested readers there are a number of excellent extended paper on this topic [68–80].

In Sec. II we briefly present a light-front representation of three-body systems and introduce the two types of wave functions that we will use for core nucleon. This will be followed by the formalism for the meson cloud model in Sec. III. Results and discussion will be presented in Sec. IV.

II. LIGHT-FRONT REPRESENTATION OF THE NUCLEON

Since the original work by Dirac [81] several decades ago, there has been an extensive use of light-front frame to study high-energy processes. References [82–85] present more in depth study of the subject for the interested reader. Now, basic definitions and formalism [86,87]. A four-vector in light-front frame is defined as

$$a = (a^+, a_-, a_\perp), \tag{1}$$

where $a^\pm = (a^\circ \pm a^3)/\sqrt{2}$ and $a_\perp = (a^1, a^2)$. Following the relativistic treatment of the nucleon by Terent'ev and coworkers [88,89], we separate the center of mass motion of the three quarks in nucleon from their relative motion by transforming their momenta p_1, p_2, p_3 into total and relative momenta as follows:

$$\vec{P} = \vec{p}_1 + \vec{p}_2 + \vec{p}_3, \tag{2a}$$

$$\xi = \frac{p_1^+}{p_1^+ + p_2^+}, \quad \eta = \frac{p_1^+ + p_2^+}{P^+}, \tag{2b}$$

$$q_\perp = (1-\xi)p_{1\perp} - \xi p_{2\perp}, \quad Q_\perp = (1-\eta)(p_{1\perp} + p_{2\perp}) - \eta p_{3\perp}. \tag{2c}$$

Then, the Hamiltonian of the system takes the form

$$H = \frac{P_\perp^2 + \hat{M}^2}{2P^+}, \tag{3}$$

where $\hat{M}$ is the mass operator with the interaction term W:

$$\hat{M} = M + W, \tag{4a}$$

$$M^2 = \frac{Q_\perp^2}{\eta(1-\eta)} + \frac{M_3^2}{\eta} + \frac{m_3^2}{1-\eta}, \tag{4b}$$

$$M_3^2 = \frac{q_\perp^2}{\xi(1-\xi)} + \frac{m_1^2}{\xi} + \frac{m_3^2}{1-\xi}, \tag{4c}$$

with m_1, m_2, and m_3 as the constituent quarks masses. M and M_3 can be rewritten in a more transparent way in terms of the relative momenta q and Q,

$$E_1 = \sqrt{\mathbf{q}^2 + m_1^2}, \quad E_2 = \sqrt{\mathbf{q}^2 + m_2^2}, \quad E_3 = \sqrt{\mathbf{Q}^2 + m_3^2}, \quad E_{12} = \sqrt{\mathbf{Q}^2 + M_3^2}, \tag{5a}$$

$$\xi = \frac{E_1 + q_3}{E_1 + E_2}, \quad \eta \frac{E_{12} + Q_3}{E_{12} + E_3}, \tag{5b}$$

$$M = E_{12} + E_3, \quad M_3 = E_1 + E_2, \tag{5c}$$

where $\mathbf{q}=(q_1, q_2, q_3)$ and $\mathbf{Q}=(Q_1, Q_2, Q_3)$.

The wave function of the nucleon can be written as

$$\Psi = \Phi\chi\phi, \tag{6}$$

where Φ, χ, and ϕ are the flavor, spin, and momentum distributions, respectively. We are going to consider two different wave functions for the core nucleon. First, assume that the nucleon is a quark-diquark system. In general, the nucleon state can be a linear combination of the following spin-isospin diquark states: (0,0), (0,1), (1,0), and (1,1). However, work done by Close [90] and Glashow and co-workers [91] suggest that the spin-zero diquark state will be the dominant one and therefore in the following we will only consider linear combination of spin-isospin diquark states (0,0) and (0,1). Therefore, the proton wave function can be written as

$$\Psi_1 = \frac{A}{\sqrt{2}}[uud(\chi^{\rho 1}\phi_1^{\lambda 1} + \chi^{\rho 2}\phi_1^{\lambda 2}) - udu(\chi^{\rho 1}\phi_1^{\lambda 1} - \chi^{\rho 3}\phi_1^{\lambda 3}) - duu(\chi^{\rho 2}\phi_1^{\lambda 2} + \chi^{\rho 3}\phi_1^{\lambda 3})] + \frac{B}{\sqrt{6}}[uud(\chi^{\rho 1}\phi_1^{\rho 1} + \chi^{\rho 2}\phi_1^{\rho 2} - 2\chi^{\rho 3}\phi_1^{\rho 3}) + udu(\chi^{\rho 1}\phi_1^{\rho 1} - 2\chi^{\rho 2}\phi_1^{\rho 2} + \chi^{\rho 3}\phi_1^{\rho 3}) + duu(-2\chi^{\rho 1}\phi_1^{\rho 1} + \chi^{\rho 2}\phi_1^{\rho 2} + \chi^{\rho 3}\phi_1^{\rho 3})]. \tag{7a}$$

For the second case we assume that there is no clustering of the quarks inside the nucleon [86]:

$$\Psi_2 = \frac{-1}{\sqrt{3}}(uud\chi^{\lambda 3} + udu\chi^{\lambda 2} + duu\chi^{\lambda 1})\phi_2. \tag{7b}$$

In Eq. (7a), $|A|^2 + |B|^2 = 1$ and in our case, with $B = -0.2$. Also, in Eq. (7), u and d represent the up and down flavors. χ^{ρ_i} and χ^{λ_i} with $i = 1, 2, 3$ represent the Melosh transformed spin wave functions [92], for example,

$$\chi_\uparrow^{\rho 3} = \frac{1}{\sqrt{2}}(\uparrow\downarrow\uparrow - \downarrow\uparrow\uparrow), \tag{8a}$$

$$\chi_\downarrow^{\rho 3} = \frac{1}{\sqrt{2}}(\uparrow\downarrow\downarrow - \downarrow\uparrow\downarrow), \tag{8b}$$

$$\chi_\uparrow^{\lambda 3} = \frac{1}{\sqrt{6}}(\downarrow\uparrow\uparrow + \uparrow\downarrow\uparrow - 2\uparrow\uparrow\downarrow), \tag{8c}$$

$$\chi_\downarrow^{\lambda 3} = \frac{1}{\sqrt{6}}(2\downarrow\downarrow\uparrow - \downarrow\uparrow\downarrow - \uparrow\downarrow\downarrow). \tag{8d}$$

The spin wave function of the ith quark is

$$\uparrow = R_i\begin{pmatrix}1\\0\end{pmatrix}, \quad \downarrow = R_i\begin{pmatrix}0\\1\end{pmatrix}. \tag{9}$$

In Eq. (9), R_i are the Melosh matrices,

$$R_1 = \frac{1}{\sqrt{a^2 + Q_\perp^2}\sqrt{c^2 + q_\perp^2}}\begin{pmatrix} ac - q_R Q_L & -aq_L - cQ_L \\ cQ_R + aq_R & ac - q_L Q_R \end{pmatrix}, \tag{10a}$$

$$R_2 = \frac{1}{\sqrt{a^2 + Q_\perp^2}\sqrt{d^2 + q_\perp^2}}\begin{pmatrix} ad + q_R Q_L & -aq_L - dQ_L \\ dQ_R - aq_R & ad - q_L Q_R \end{pmatrix}, \tag{10b}$$

$$R_3 = \frac{1}{\sqrt{b^2 + Q_\perp^2}}\begin{pmatrix} b & Q_L \\ -Q_R & b \end{pmatrix}, \tag{10c}$$

where

$$a = M_3 + \eta M, \quad b = m_3 + (1-\eta)M, \tag{11a}$$

$$c = m_1 + \xi M_3, \quad d = m_2 + (1-\xi)M_3, \tag{11b}$$

$$q_R = q_1 + iq_2, \quad q_L = q_1 - iq_2, \tag{11c}$$

$$Q_R = Q_1 + iQ_2, \quad Q_L = Q_1 - iQ_2. \tag{11d}$$

The functions $\phi_1^{\rho i}$ and $\phi_1^{\lambda i}$, with $i=1,2,3$, and ϕ_2 are the momentum wave functions, which we take them to be of the following form:

$$\phi_1^{\rho i} = N_{\rho i}(X_j - X_k)\phi_1^{si}/X_T, \tag{12a}$$

$$\phi_1^{\lambda i} = N_{\lambda i}(X_j + X_k - 2X_i)\phi_1^{si}/X_T, \tag{12b}$$

with $i \neq j \neq k$, and [86]

$$\phi_2 = \frac{N}{(M^2+\beta^2)^{3.5}}. \tag{12c}$$

Also,

$$X_3 = \frac{Q_\perp^2}{2\eta(1-\eta)\beta_Q^2} + \frac{q_\perp^2}{2\eta\xi(1-\xi)\beta_q^2} + \frac{m_1^2}{2\eta\xi\beta_q^2} + \frac{m_2^2}{2\eta(1-\xi)\beta_q^2} + \frac{m_3^2}{2(1-\eta)\beta_Q^2}, \tag{13a}$$

$$X_2 = q_\perp^2 \frac{(1-\eta)(1-\xi)\beta_Q^2 + \xi\beta_q^2}{2\beta_Q^2\beta_q^2\eta\xi(1-\xi)(1-\eta+\xi\eta)} + Q_\perp^2 \frac{(1-\xi)(1-\eta)\beta_q^2 + \xi\beta_Q^2}{2\beta_Q^2\beta_q^2\eta(1-\eta)(1-\eta+\xi\eta)} + q_\perp Q_\perp \frac{\beta_Q^2 - \beta_q^2}{\beta_Q^2\beta_q^2\eta(1-\eta+\xi\eta)} + \frac{m_1^2}{2\eta\xi\beta_q^2} + \frac{m_2^2}{2\eta(1-\xi)\beta_Q^2} + \frac{m_3^2}{2(1-\eta)\beta_q^2}, \tag{13b}$$

$$X_1 = q_\perp^2 \frac{(1-\xi)\beta_q^2 + \xi(1-\eta)\beta_Q^2}{2\beta_Q^2\beta_q^2\eta\xi(1-\xi)(1-\xi\eta)} + Q_\perp^2 \frac{(1-\xi)\beta_Q^2 + \xi(1-\eta)\beta_q^2}{2\beta_Q^2\beta_q^2\eta(1-\xi)(1-\xi\eta)} - q_\perp Q_\perp \frac{\beta_Q^2 - \beta_q^2}{\beta_Q^2\beta_q^2\eta(1-\xi\eta)} + \frac{m_1^2}{2\eta\xi\beta_Q^2} + \frac{m_2^2}{2\eta(1-\xi)\beta_q^2} + \frac{m_3^2}{2(1-\eta)\beta_q^2}, \tag{13c}$$

$$X_T = X_1 + X_2 + X_3, \tag{13d}$$

and

$$\phi_1^{si} = \frac{1}{(1+X_T)^{ni}}. \tag{13e}$$

In the above equations β_Q, β_q, and β are confinement scale parameters and N_{ρ_i}, N_{λ_i}, and N are normalization constants.

III. MESON CLOUD MODEL IN LIGHT-CONE FRAME

Meson cloud model has been used extensively in the 1990s, mostly to investigate the flavor asymmetry of the nucleon sea. In this approach using the convolution model, one can decompose the physical nucleon in terms of the core nucleon and intermediate, virtual meson-baryon states [2–35]. Following the work done by Zoller [12], Holtmann, Szczurek, and Speth [32], and Speth and Thomas [33], one can write

$$|N\uparrow\rangle = Z^{1/2}\left[|N\uparrow\rangle_{bare} + \sum_{BM}\sum_{\lambda\lambda'}\int dy d^2k_\perp \beta_{BM}^{\lambda\lambda'}(y,k_\perp^2) \times |B^\lambda(y,\vec{k}_\perp); M^{\lambda'}(1-y,-\vec{k}_\perp)\rangle\right], \tag{14a}$$

with

$$\beta_{BM}^{\lambda\lambda'}(y,k_\perp^2) = \frac{1}{2\pi\sqrt{y(1-y)}} \frac{\sqrt{m_N m_B}V_{IMF}^{\lambda\lambda'}(y,k_\perp^2)}{m_N^2 - M_{BM}^2(y,k_\perp^2)}, \tag{14b}$$

where Z is the probability of the physical nucleon being in the core state. $\beta_{BM}^{\lambda\lambda'}(y,k_\perp^2)$ is the probability amplitude for the physical nucleon with helicity $+\frac{1}{2}$ is in a virtual state consisting of baryon $B^\lambda(y,\vec{k}_\perp)$, with helicity λ, longitudinal momentum y, and transverse momentum $\vec{k}_\perp$, and meson $M^{\lambda'}(1-y,-\vec{k})$, with helicity λ', longitudinal momentum $1-y$ and transverse momentum $-\vec{k}$. $V_{IMF}^{\lambda\lambda'}(y,k_\perp^2)$, is the vertex function and its explicit form for different baryon-meson pairs with their corresponding helicities are listed in the Appendix. The summations in Eq. (14a) and (14b) include all physically possible pairs from the pseudoscalar and vector mesons and their corresponding baryons from baryon octet and decuplet. Using $\beta_{BM}^{\lambda\lambda'}(y,k_\perp^2)$, one can define polarized splitting function in the following way:

$$n_{BM/N}^\lambda(y) = \sum_{\lambda'}\int_0^\infty dk_\perp^2 |\beta_{BM}^{\lambda\lambda'}(y,k_\perp^2)|^2, \tag{15a}$$

TABLE I. Parameters used in set 1 and 2. Here m_u, m_d, β_Q, and β_q are all in GeV, and μ_p and μ_n are in nuclear magneton units. Set 1 represents our diquark-quark model, while set 2 represents parameters used by Schlumpf [86,87].

	m_u	m_d	β_Q	β_q	n_1	n_2	n_3	μ_p	μ_n
Set 1	0.250	0.210	0.25	0.45	2.8	2.8	2.6	2.82	−1.61
Set 2	0.263	0.263	0.607	0.607	3.5	3.5	3.5	2.81	−1.66

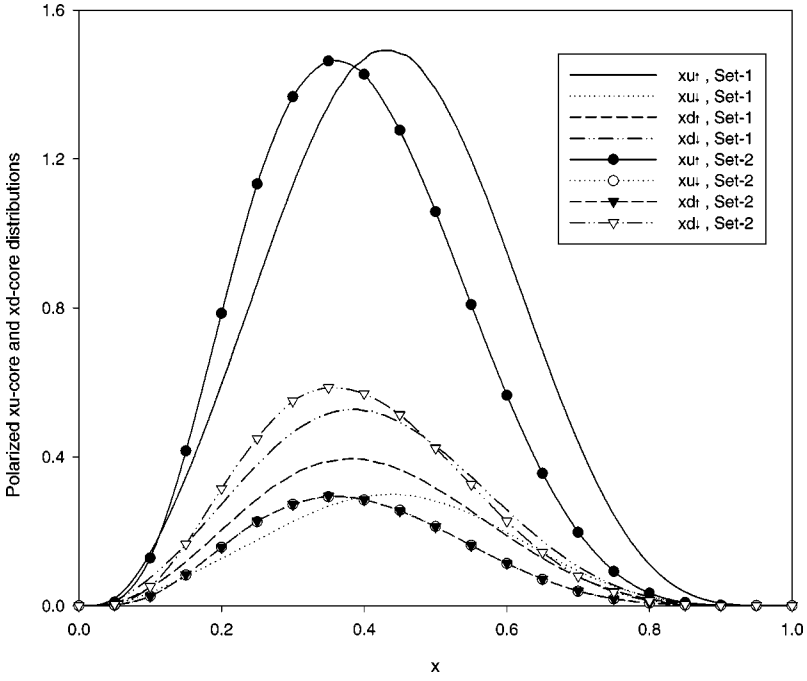

FIG. 1. Polarized *xu*-core and *xd*-core distributions for sets 1 and 2. Set 1 represents a diquark-quark distribution while in set 2 there is no quark clustering.

$$n^{\lambda'}_{MB/N}(y) = \sum_{\lambda} \int_0^{\infty} dk_\perp^2 |\beta^{\lambda\lambda'}_{BM}(1-y, k_\perp^2)|^2. \qquad (15b)$$

The splitting functions must satisfy the equations

$$n_{MB}(y) = n_{BM}(1-y) \qquad (15c)$$

and

$$\langle x n_{MB}\rangle + \langle x n_{BM}\rangle = \langle n_{BM}\rangle. \qquad (15d)$$

In Eq. (15d), $\langle n\rangle$ and $\langle xn\rangle$ are the first and second moments of the splitting functions. Equation (15c) ensures the global charge conservation and Eq. (15d) momentum conservation.

Calculation of the physical polarized quark distributions is basically the same as what was done in Refs. [1,2]. Namely, the polarized core quark distribution can be written [93] as:

$$q^{\lambda}_{core}(x) = \sum_j \langle N\uparrow | P^j_{q^\lambda} \delta(x - x_j) | N\uparrow\rangle, \qquad (16a)$$

$$= 3\langle N\uparrow | P^3_{q^\lambda} \delta(x - x_3) | N\uparrow\rangle, \qquad (16b)$$

with

$$\sum_i x_i = 1, \qquad (16c)$$

where $x_1 = \xi\eta$, $x_2 = \eta(1-\xi)$, and $x_3 = 1-\eta$, and $P^j_{q^\lambda}$ is a projection operator that projects out jth quark with helicity λ

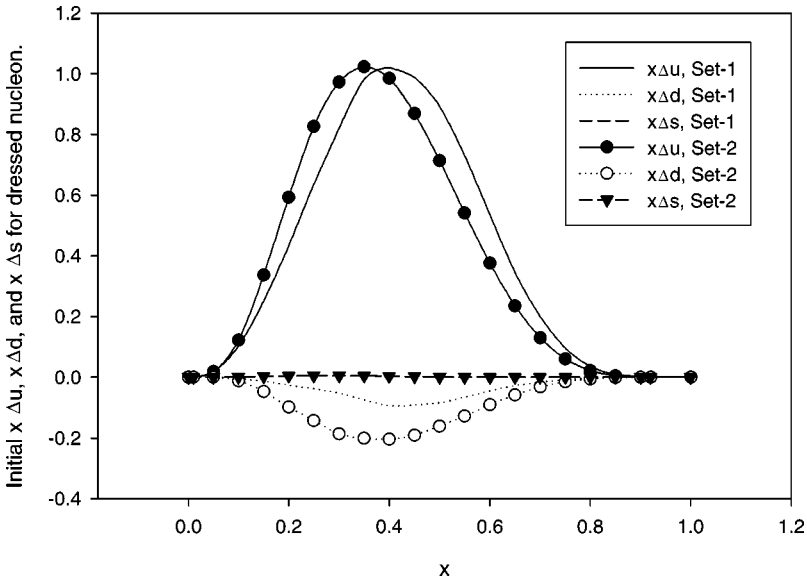

FIG. 2. Initial $x\Delta u$, $x\Delta d$, and $x\Delta s$ for dressed nucleon. Set 1 represents a diquark-quark distribution while in set 2 there is no quark clustering.

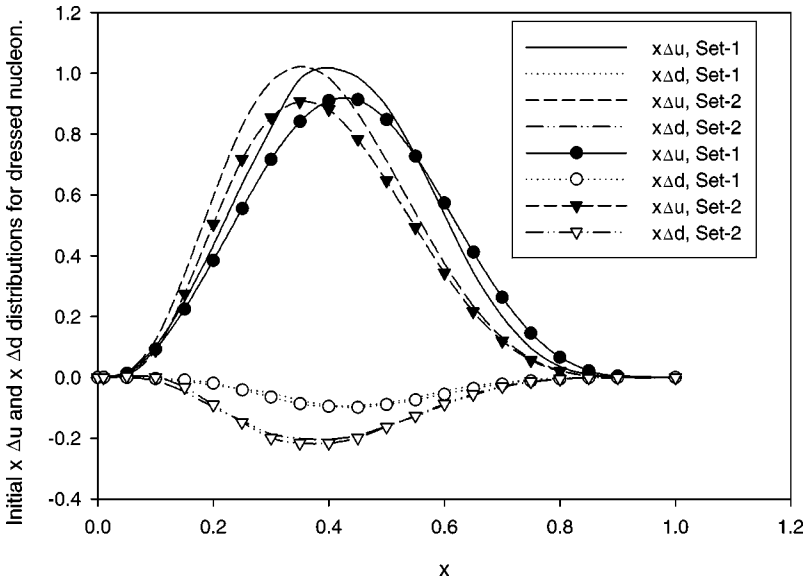

FIG. 3. Initial $x\Delta u$ and $x\Delta d$ distributions for dressed nucleon. The line curves include both vector and pseudoscalar meson contributions, while the line-symbol curves include only the pseudoscalar contribution from Ref. [2]. Set 1 represents a diquark-quark distribution but in set 2 there is no quark clustering.

and Eq. (16b) is for symmetrized wave function. For pseudoscalar and vector meson distributions we have used the formulation in Refs. [94] and [95], respectively. Using the core quark distribution along with the meson cloud and their companion baryons one can obtain the initial quark distributions [2].

These initial distributions are calculated at some initial low Q_0^2. In order to be able to compare our results with experiments, we evolve these initial distributions using DGLAP equations [96–98] to some final high Q^2. The DGLAP equations for polarized distributions are [69]

$$\frac{d}{dt}\Delta q_{NS}(x,t) = \frac{\alpha_s(t)}{2\pi}\Delta P_{qq}^{NS}(x) \otimes \Delta q_{NS}(x,t) \qquad (17a)$$

for nonsinglet distributions and

$$\frac{d}{dt}\Delta q_S(x,t) = \frac{\alpha_s(t)}{2\pi}[\Delta P_{qq}^{S}(x) \otimes \Delta q_S(x,t) + 2n_f \Delta P_{qG}(x) \otimes \Delta G(x,t)], \qquad (17b)$$

$$\frac{d}{dt}\Delta G(x,t) = \frac{\alpha_s(t)}{2\pi}[\Delta P_{Gq}^{S}(x) \otimes \Delta q_S(x,t) + \Delta P_{GG}(x) \otimes \Delta G(x,t)] \qquad (17c)$$

for singlet distributions. In Eq. (17) α_s is the QCD running coupling constant Δq and ΔG are the polarized quark and gluon distribution functions, ΔPs are the splitting functions, f is the number of flavors, and t is defined as

$$t = \ln(Q^2/Q_0^2). \qquad (17d)$$

Having the polarized distribution functions one can calculate polarized singlet, a_0, and nonsinglet, a_3 and a_8, distributions and polarized structure functions g_1^p and g_1^n along with their first moment in the following way:

$$a_0(x) = \Delta u(x) + \Delta d(x) + \Delta s(x), \qquad (18a)$$

$$a_3(x) = \Delta u(x) - \Delta d(x), \qquad (18b)$$

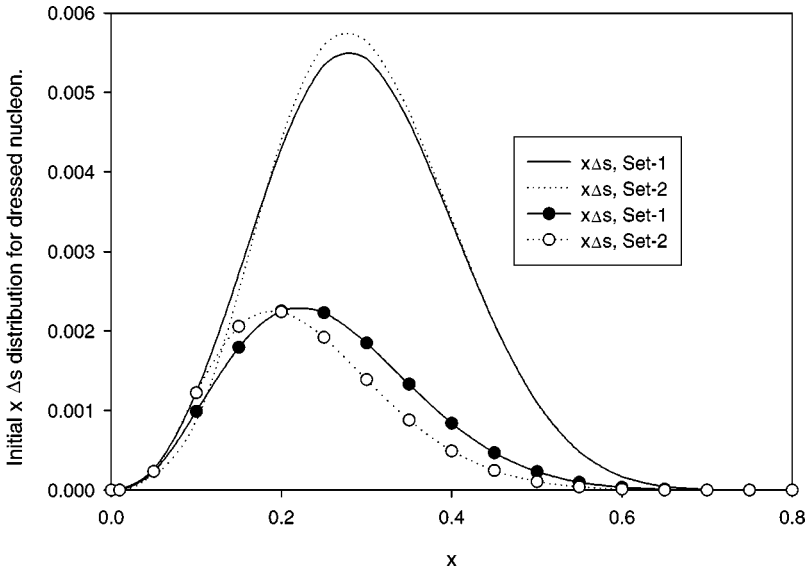

FIG. 4. Initial $x\Delta s$ distributions for dressed nucleon. The line curves include both vector and pseudoscalar meson contributions, while the line-symbol curves include only the pseudoscalar contribution from Ref. [2]. Set 1 represents a diquark-quark distribution but in set 2 there is no quark clustering.

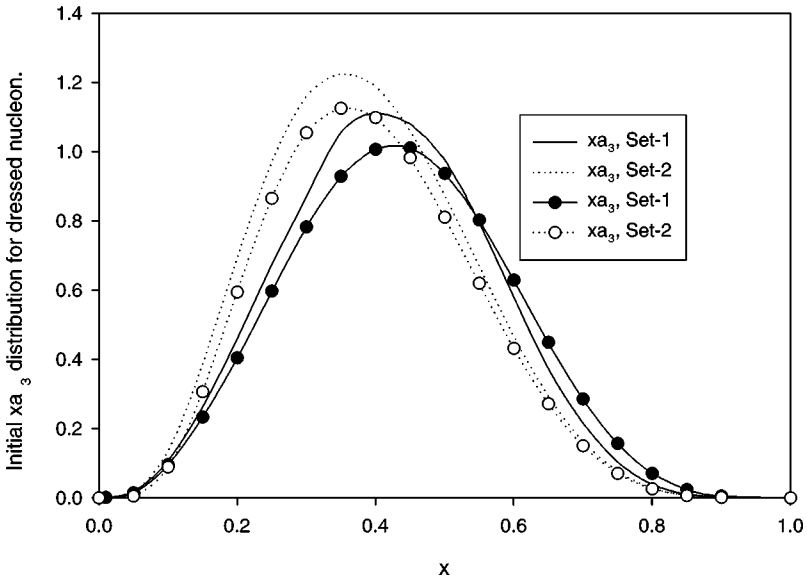

FIG. 5. Initial xa_3 distributions for dressed nucleon. The line curves include both vector and pseudoscalar meson contributions, while the line-symbol curves include only the pseudoscalar contribution from Ref. [2]. Set 1 represents a diquark-quark distribution but in set 2 there is no quark clustering.

$$a_8(x) = \frac{\Delta u(x) + \Delta d(x) - 2\Delta s(x)}{\sqrt{3}}, \tag{18c}$$

$$g_1^p(x) = \frac{1}{2}\left(\frac{4}{9}\Delta u(x) + \frac{1}{9}\Delta d(x) + \frac{1}{9}\Delta s(x)\right), \tag{18d}$$

$$g_1^n(x) = \frac{1}{2}\left(\frac{1}{9}\Delta u(x) + \frac{4}{9}\Delta d(x) + \frac{1}{9}\Delta s(x)\right), \tag{18e}$$

where

$$\Delta q(x) = [q_\uparrow(x) - q_\downarrow(x)] + [\bar{q}_\uparrow(x) - \bar{q}_\downarrow(x)], \tag{18f}$$

also,

$$\Gamma_1^p = \int_0^1 g_1^p(x)dx, \tag{19a}$$

$$\Gamma_1^n = \int_0^1 g_1^n(x)dx, \tag{19b}$$

where Eq. (19) represents the first moment of $g_1^p(x)$ and $g_1^n(x)$. Using Eqs. (18) and (19) one can calculate BSR [61,62] and EJSR [63]:

$$S_B = \Gamma_1^p - \Gamma_1^n, \tag{20a}$$

$$S_{EJ}^p = \frac{1}{12}\left(a_3 + \frac{5}{\sqrt{3}}a_8\right), \tag{20b}$$

$$S_{EJ}^n = \frac{1}{12}\left(-a_3 + \frac{5}{\sqrt{3}}a_8\right). \tag{20c}$$

Using Eqs. (18a)–(18c) one could write polarized quark distributions in terms of singlet and nonsinglet distributions:

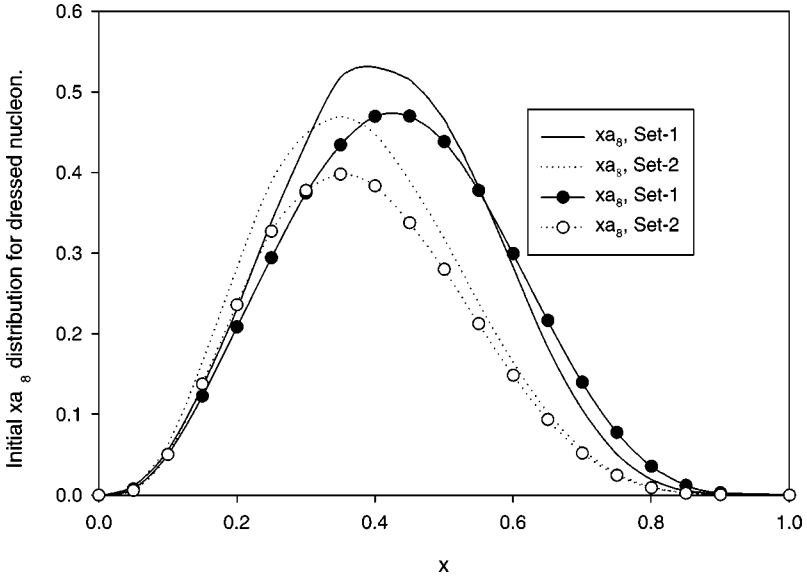

FIG. 6. Initial xa_8 distributions for dressed nucleon. The line curves include both vector and pseudoscalar meson contributions, while the line-symbol curves include only the pseudoscalar contribution from Ref. [2]. Set 1 represents a diquark-quark distribution but in set 2 there is no quark clustering.

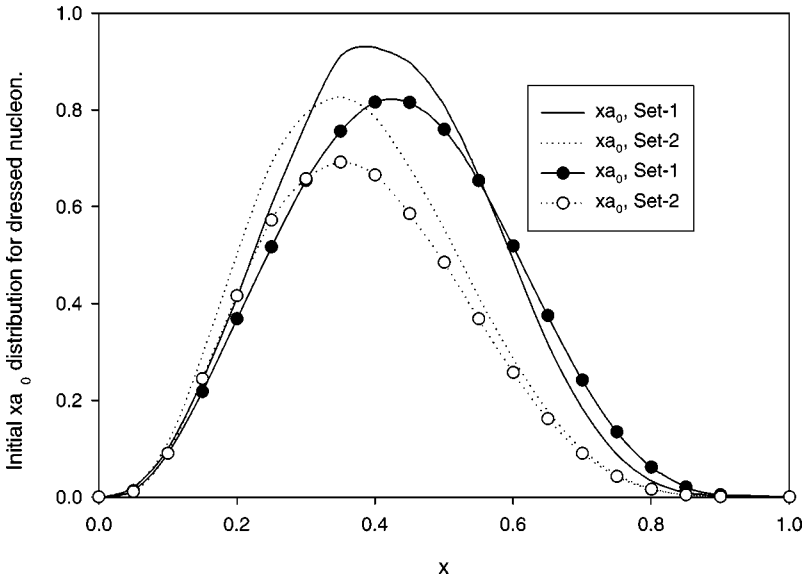

FIG. 7. Initial xa_0 distributions for dressed nucleon. The line curves include both vector and pseudoscalar meson contributions, while the line-symbol curves include only the pseudoscalar contribution from Ref. [2]. Set 1 represents a diquark-quark distribution but in set 2 there is no quark clustering.

$$\Delta u = \frac{(\sqrt{3}a_8 + 2a_0 + 3a_3)}{6}, \tag{21a}$$

$$\Delta d = \frac{(\sqrt{3}a_8 + 2a_0 - 3a_3)}{6}, \tag{21b}$$

$$\Delta s = \frac{(-\sqrt{3}a_8 + a_0)}{3}. \tag{21c}$$

IV. RESULTS AND DISCUSSION

In Table I we present the parameters, in energy units of GeV, that have been used in Eqs. (12), (13), (16), and (17) to calculate quark distribution functions and the proton and neutron polarized structure functions. Set 1 represents diquark-quark distribution dominated by the isoscalar diquark for the core nucleon. Set 2 is the parameters used by Schlumpf [86] and represent symmetrical distribution of quarks inside the nucleon.

In Fig. 1 we present polarized xu and xd distributions for the core nucleon. One can see the relative closeness of $d_\uparrow$ and $d_\downarrow$ for the diquark-quark distribution, which means rather small magnitude of Δd for set 1. Having these distributions the bare nucleon is dressed up into physical nucleon by introducing the meson cloud at some initial low momentum transferred. Figure 2 shows $x\Delta u$, $x\Delta d$, and $x\Delta s$ distributions for sets 1 and 2. Couple of points concerning this graph, one that Δd is significantly larger for set 2 compared with that of Set 1 and the second one is the rather smallness of Δs for both sets which is expected. In Fig. 3 we compare the results of the present calculations of $x\Delta u$ and $x\Delta d$ with that of Ref. [2] to show the impact of the vector mesons on u and d quark polarization. One can see that there is a noticeable increase in u-quark polarization and a reduction of difference between sets 1 and 2 compared with that of Ref. [2]. For d quark, at

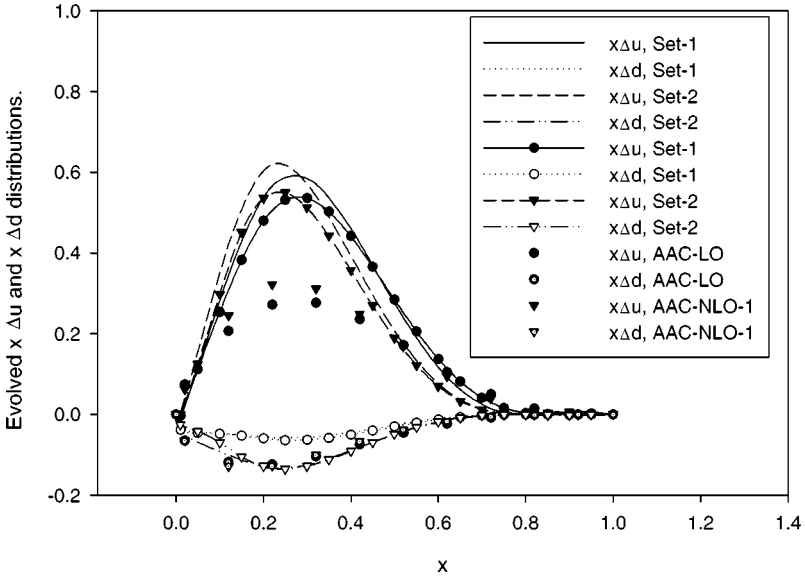

FIG. 8. Evolved $x\Delta u$ and $x\Delta d$ distributions with corrections due to gluon anomaly. The line curves include both vector and pseudoscalar meson contributions, while the line-symbol curves include only the pseudoscalar contribution from Ref. [2]. The symbols AAC-LO and AAC-NLO-1 have been generated using leading order and next-to-leading order calculations by AAC group, respectively (Ref. [101]). Set 1 represents a diquark-quark distribution but in set 2 there is no quark clustering.

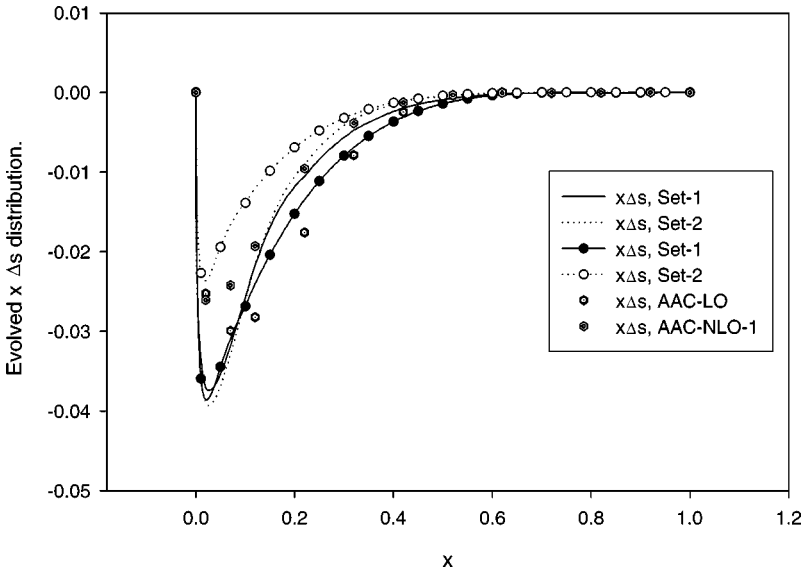

FIG. 9. Evolved $x\Delta s$ distributions with corrections due to gluon anomaly. The line curves include both vector and pseudoscalar meson contributions, while the line-symbol curves include only the pseudoscalar contribution from Ref. [2]. The symbols AAC-LO and AAC-NLO-1 have been generated using leading order and next-to-leading order calculations by AAC group, respectively (Ref. [101]). Set 1 represents a diquark-quark distribution but in set 2 there is no quark clustering.

small x (i.e., $x\sim 0.1$), there is slight increase in magnitude of polarization, while for medium x there is slight decrease in polarization. Figure 4 represents comparison of s-quark polarization. The first point to be made is that all distributions are positive, in contrast with the observation (see, for example, Ref. [53]). However, this is not surprising since we have not introduced any gluon polarization at this stage. At this point we would like to mention that one can correctly infer that our model does predict asymmetries between the strange and antistrange quark distributions. However, we have shown in Ref. [3] that $\int_0^1 [s(x)+\bar{s}(x)]dx=0$ as it should be for the nucleon. Finally, in Fig. 4 one can see a significant increase in s-quark polarization and a reduction of difference between sets 1 and 2. Figures 5–7 present the comparison of xa_3, xa_8, and xa_0 of the present work with that of Ref. [2]. One can see the effect of the dominance of u quark in the quark model; namely, a noticeable increase in all three distributions, which is in accord with the results of Fig. 3. These initial distributions are evolved using the code of Kumano and co-workers [99,100] to final momentum transferred and compared with experimental results. The code uses the modified minimal subtraction ($\overline{MS}$) renormalization scheme and calculates Q^2 evolution to the next-to-leading order of the running coupling constant with QCD scale parameter of 0.2 GeV. To be consistent we have used the same evolution parameter as Ref. [2], namely, $t=0.3$, and have assumed that there is no initial gluon polarization. However, evolution generates gluon polarization. In set 1 we get $\Delta G=0.78$ and in set 2 we get $\Delta G=0.76$, which are much closer compared to those in Ref. [2]. For the sake of consistency we renormalize total gluon polarization for both sets to be 2.5. Although, this seems to be a rather high contribution, it is not unexpected in pQCD but it should be considered as absolute upper limit as explained by Ellis and Karliner [70]. As mentioned in the Introduction, the experimental observation is actually a superposition of quark and gluon polarizations. Taking this into account, one can write

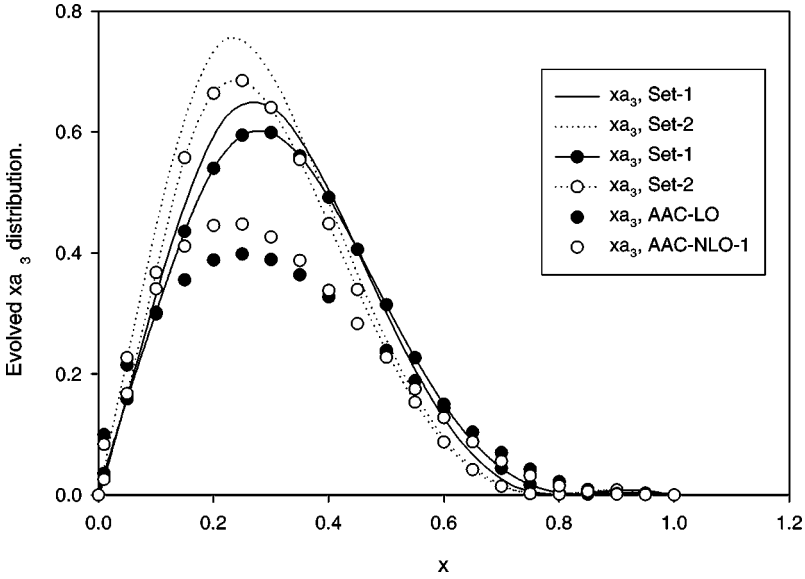

FIG. 10. Evolved xa_3 distributions with corrections due to gluon anomaly. The line curves include both vector and pseudoscalar meson contributions, while the line-symbol curves include only the pseudoscalar contribution from Ref. [2]. The symbols AAC-LO and AAC-NLO-1 have been generated using leading order and next-to-leading order calculations by AAC group, respectively (Ref. [101]). Set 1 represents a diquark-quark distribution but in set 2 there is no quark clustering.

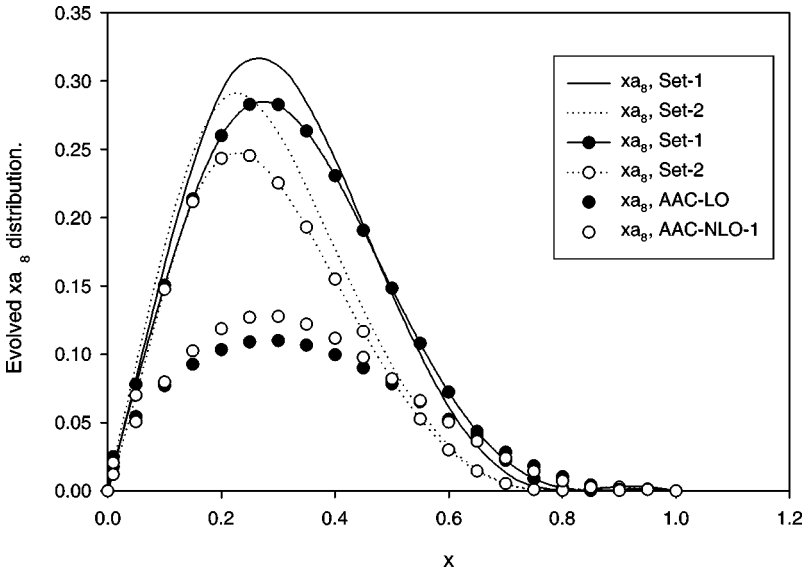

FIG. 11. Evolved xa_8 distributions with corrections due to gluon anomaly. The line curves include both vector and pseudoscalar meson contributions, while the line-symbol curves include only the pseudoscalar contribution from Ref. [2]. The symbols AAC-LO and AAC-NLO-1 have been generated using leading order and next-to-leading order calculations by AAC group, respectively (Ref. [101]). Set 1 represents a diquark-quark distribution but in set 2 there is no quark clustering.

$$\Delta q \rightarrow \Delta q - \frac{\alpha_s}{2\pi}\Delta G, \tag{22}$$

where α_s is QCD running coupling constant and in our case we choose $\alpha_s/2\pi=0.048$ which relates to Q^2 of about 4 GeV^2. The results of taking into account Eq. (22) for evolved distributions are shown in Figs. 8–12. To avoid overcrowding the graphs, instead of comparing our work with several experimental data, we compare our work with the best fit to world experimental data by the AAC Group [101]. As expected, the evolution results in the shift of the distribution peaks to lower x. Also, the inclusion of gluon anomaly leads to a very good agreement of polarized strange quark distribution with observation as can be seen in Fig. 9. Since the addition of the vector mesons lead to increase in u-quark polarization, one can see from Figs. 8 and 10–12 that set 2 of pseudoscalar leads to the best agreement with experimental data for $x\Delta u$, xa_3, xa_8, and xa_0, respectively. However, for Δd and Δs, one can see from Figs. 8 and 9, respectively, that the addition of the vector mesons leads to better agreement with observation. Our numerical results along with some experimental and theoretical results are presented in Table II. There are few points to be made concerning this data. Set 1 even after introduction of gluon anomaly results in rather small magnitude of Δd and positive first moment of g_1^n, which is in contrast with observation [44,51,52]. These are basically the same as those in Ref. [2]. Similarly, as in Ref. [2], set 1 reproduces strange quark polarization and BSR rather nicely. For set 2, there is rather a significant difference between the current work and that of Ref. [2]. The results for Δd and g_1^n are much better compared with Ref. [2]. However, that is not the case for BSR, namely, it overestimates BSR by even a larger margin. But like set 1, set 2 reproduces Δs rather nicely. The important point is that when one compares the last four rows of Table II with other theoretical calculations (rows 5 and 6), one realizes that introduction of meson cloud in relativistic quark

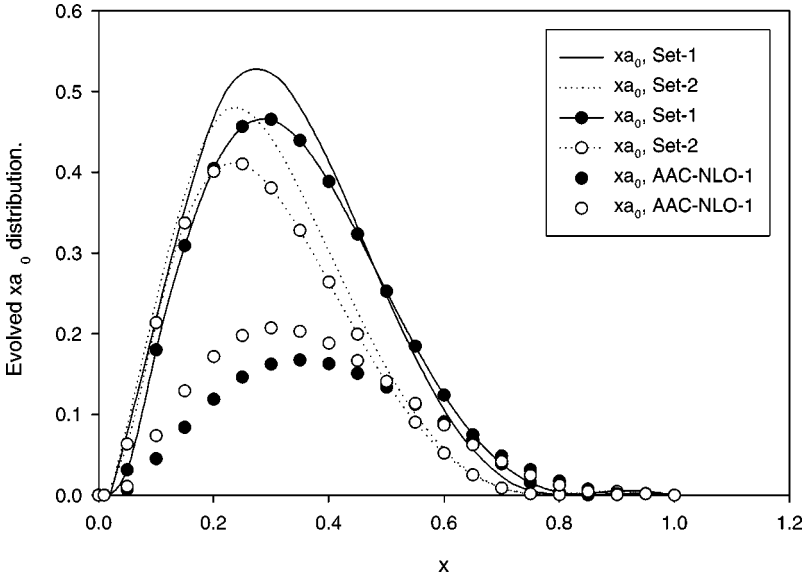

FIG. 12. Evolved xa_0 distributions with corrections due to gluon anomaly. The line curves include both vector and pseudoscalar meson contributions, while the line-symbol curves include only the pseudoscalar contribution from Ref. [2]. The symbols AAC-LO and AAC-NLO-1 have been generated using leading order and next-to-leading order calculations by AAC group, respectively (Ref. [101]). Set 1 represents a diquark-quark distribution but in set 2 there is no quark clustering.

TABLE II. Comparison of the results of our models with theory and experiment. The first three rows are experimental results corresponding to Refs. [52], [53], and [44] respectively. The fourth row corresponds to Ellis-Jaffe [63] and Bjorken [61,62] sum rules. The fifth row is simply the nonrelativistic quark parton model prediction. The sixth row corresponds to relativistic quark model calculations [104]. The results of our work are presented in the last six rows.

	Δu	Δd	Δs	Γ_1^p	Γ_1^n	$\Gamma_1^p-\Gamma_1^n$
E143 (3 GeV^2)	0.83	−0.43	−0.09	0.133	−0.032	0.165
E154 (5 GeV^2)				0.122	−0.056	0.168
SMC (5 GeV^2)				0.132	−0.048	0.181
EJSR/BSR				0.167	−0.015	0.182
NRQPM (ΔG=0)	1.33	−0.33	0			
RQPM (ΔG=0)	1.0	−0.25	0			
Set 1 (ΔG=0, Ref. [2])	1.04	−0.075	0.015	0.228	0.042	0.186
Set 2 (ΔG=0, Ref. [2])	1.02	−0.199	0.014	0.216	0.013	0.203
Set 1 ($\Delta G \neq 0$, Ref. [2])	0.917	−0.195	−0.105	0.187	0.002	0.185
Set 2 ($\Delta G \neq 0$, Ref. [2])	0.951	-0.271	−0.059	0.193	−0.011	0.204
Set 1 ($\Delta G \neq 0$, current work)	1.00	−0.187	−0.100	0.208	0.009	0.199
Set 2 ($\Delta G \neq 0$, current work)	1.07	−0.324	−0.101	0.213	−0.018	0.231

model results in better agreement with experiment, which once again shows the significance of the role of meson cloud in nucleon structure.

One final comment is that the addition of vector mesons did not resolve the situation that we faced in Refs. [2,3]. Namely, in Ref. [3] we calculated the F_2 structure function for the nucleon using the same approach as we have done in the present work. There we showed that a diquark-quark distribution which is dominated by an isoscalar diquark makes it possible to have reasonable agreement with experiment. In contrast with a core nucleon where there is no clusterization of quarks, the calculated F_2 structure function consistently undershoots the observation rather significantly in the medium to high x range. However, for the polarized case, with and without the vector mesons, the results are mixed for both sets. However, what all these works have in common is that how the meson cloud can be used to gain insight through the polarized and unpolarized structures of the nucleon.

APPENDIX

The explicit form of the vertex function $V_{IMF}^{\lambda\lambda'}(y,k_\perp^2)$, used in Eq. (14b) is

$$V_{IMF}^{\lambda\lambda'}(y,k_\perp^2)=|\Gamma_{MB}(M_{MB}^2)|^2 V'^{\lambda\lambda'}_{IMF}(y,k_\perp^2), \tag{A1}$$

where $\Gamma_{MB}(M_{MB}^2)$ is the vertex form factor and is parametrized by the exponential function of the invariant mass M_{MB} of the intermediate baryon-meson state:

$$\Gamma_{MB}(M_{MB}^2)=e^{-(M_{MB}^2-m_N^2)/\Lambda_{MB}^2}, \tag{A2}$$

where Λ_{MB} are free parameters which are determined by fitting experimental data. In the following we present the explicit form of $V'^{\lambda\lambda'}_{IMF}(y,k_\perp^2)$ for intermediate helicity states of pseudoscalar meson and baryon states, calculated by Holtmann and co-workers [32,33]. For intermediate states $N\pi$, $N\eta$, ΣK, and ΛK the vertex functions are

$$\frac{1}{2}\rightarrow+\frac{1}{2},\quad 0\quad \frac{g_{NMB}}{2}\frac{ym_N-m_B}{\sqrt{ym_N m_B}}, \tag{A3}$$

$$\frac{1}{2}\rightarrow-\frac{1}{2},\quad 0\quad \frac{g_{NMB}e^{-i\phi}}{2}\frac{k_\perp}{\sqrt{ym_N m_B}}. \tag{A4}$$

For $\Delta\pi, \Sigma^* K$ intermediate states we have

$$\frac{1}{2}\rightarrow+\frac{3}{2},\quad 0\quad -\frac{f_{NMB}e^{+i\phi}}{2\sqrt{2}}\frac{k_\perp(ym_N+m_B)}{y\sqrt{ym_N m_B}}, \tag{A5}$$

$$\frac{1}{2}\rightarrow+\frac{1}{2},\quad 0 \times\frac{f_{NMB}}{2\sqrt{6}}\frac{(ym_N+m_B)^2(ym_N-m_B)+k_\perp^2(ym_N+2m_B)}{ym_B\sqrt{ym_N m_B}}, \tag{A6}$$

$$\frac{1}{2}\rightarrow-\frac{1}{2},\quad 0 \times\frac{f_{NMB}e^{-i\phi}}{2\sqrt{6}}\frac{k_\perp[(ym_N+m_B)^2-3m_B(ym_N+2m_B)+k_\perp^2]}{ym_B\sqrt{ym_N m_B}}, \tag{A7}$$

$$\frac{1}{2}\rightarrow-\frac{3}{2},\quad 0-\frac{f_{NMB}e^{-2i\phi}}{2\sqrt{2}}\frac{k_\perp^2}{y\sqrt{ym_N m_B}}. \tag{A8}$$

For $N\rho, N\omega, \Sigma K^*, \Lambda K^*$ intermediate states we have

$$\frac{1}{2}\to+\frac{1}{2},\quad +1 \times\frac{g_{NMB}e^{+i\phi}}{\sqrt{2}}\frac{k_\perp}{(1-y)\sqrt{ym_Nm_B}}-f_{NMB}\sqrt{2}e^{+i\phi}\frac{k_\perp m_N}{\sqrt{ym_Nm_B}}, \tag{A9}$$

$$\frac{1}{2}\to+\frac{1}{2},\quad 0 \times\frac{g_{NMB}}{2}\frac{k_\perp^2+m_Nm_B(1-y)^2-ym_M^2}{2(1-y)m_M\sqrt{ym_Nm_B}}-\frac{f_{NMB}}{2} \times\frac{(ym_N-m_B)(y^2m_N^2-y(m_N^2+m_B^2+m_M^2)+m_B^2+k_\perp^2)}{ym_M\sqrt{ym_Nm_B}}, \tag{A10}$$

$$\frac{1}{2}\to+\frac{1}{2},\quad -1 \times\frac{g_{NMB}e^{-i\phi}}{\sqrt{2}}\frac{yk_\perp}{(1-y)\sqrt{ym_Nm_B}}+f_{NMB}\sqrt{2}e^{-i\phi}\frac{k_\perp m_B}{\sqrt{ym_Nm_B}}, \tag{A11}$$

$$\frac{1}{2}\to-\frac{1}{2},\quad +1 \times\frac{g_{NMB}}{\sqrt{2}}\frac{ym_N-m_B}{\sqrt{ym_Nm_B}} -f_{NMB}\sqrt{2}\frac{k_\perp^2-(m_N+m_B)(1-y)(ym_N-m_B)}{(1-y)\sqrt{ym_Nm_B}}, \tag{A12}$$

$$\frac{1}{2}\to-\frac{1}{2},\quad 0 -\frac{g_{NMB}e^{-i\phi}}{2}\frac{k_\perp+(m_N-m_B)}{m_M\sqrt{ym_Nm_B}}-\frac{f_{NMB}e^{-i\phi}}{2} \times\frac{k_\perp(1+y)[y^2m_N^2-y(m_N^2+m_B^2+m_M^2)+m_B^2+k_\perp^2]}{y(1-y)m_M\sqrt{ym_Nm_B}}, \tag{A13}$$

$$\frac{1}{2}\to+\frac{1}{2},\quad -1\quad f_{NMB}\sqrt{2}e^{-2i\phi}\frac{k_\perp^2}{(1-y)\sqrt{ym_Nm_B}}. \tag{A14}$$

Finally, for $\Delta\rho,\Sigma^*K^*$ we have

$$\frac{1}{2}\to+\frac{3}{2},\quad +1\quad -\frac{f_{NMB}e^{+2i\phi}}{2}\frac{k_\perp}{y(1-y)\sqrt{ym_Nm_B}}, \tag{A15}$$

$$\frac{1}{2}\to+\frac{3}{2},\quad 0\quad \frac{f_{NMB}e^{+i\phi}}{\sqrt{2}}\frac{k_\perp m_N}{(1-y)\sqrt{ym_Nm_B}}, \tag{A16}$$

$$\frac{1}{2}\to+\frac{3}{2},\quad -1\quad \frac{f_{NMB}}{2}\frac{m_Nm_B(1-y)^2-ym_M^2}{(1-y)\sqrt{ym_Nm_B}}, \tag{A17}$$

$$\frac{1}{2}\to+\frac{1}{2},\quad +1\quad \frac{f_{NMB}e^{+i\phi}}{2\sqrt{3}}\frac{k_\perp[k_\perp^2-2(1-y)m_B^2]}{y(1-y)m_B\sqrt{ym_Nm_B}}, \tag{A18}$$

$$\frac{1}{2}\to+\frac{1}{2},\quad 0\quad -\frac{f_{NMB}}{\sqrt{6}}\frac{m_M[k_\perp^2+m_B(1-y)(ym_N-m_B)]}{(1-y)m_B\sqrt{ym_Nm_B}}, \tag{A19}$$

$$\frac{1}{2}\to+\frac{1}{2},\quad -1\quad \frac{f_{NMB}e^{-i\phi}}{2\sqrt{3}}\frac{k_\perp[ym_M^2-2m_Nm_B(1-y)]}{(1-y)m_B\sqrt{ym_Nm_B}}, \tag{A20}$$

$$\frac{1}{2}\to-\frac{1}{2},\quad +1 \times\frac{f_{NMB}e^{-i\phi}}{2\sqrt{3}}\frac{2(1-y)m_Bk_\perp^2+m_Nm_M^2y^3-(1-y)^2m_B^3}{y(1-y)m_B\sqrt{ym_Nm_B}}, \tag{A21}$$

$$\frac{1}{2}\to-\frac{1}{2},\quad 0\quad \frac{f_{NMB}e^{-i\phi}}{\sqrt{6}}\frac{k_\perp m_M[ym_N-(1-y)m_B]}{(1-y)m_B\sqrt{ym_Nm_B}}, \tag{A22}$$

$$\frac{1}{2}\to-\frac{1}{2},\quad -1\quad \frac{f_{NMB}e^{-2i\phi}}{2\sqrt{3}}\frac{k_\perp^2m_N}{(1-y)m_B\sqrt{ym_Nm_B}}, \tag{A23}$$

$$\frac{1}{2}\to-\frac{3}{2},\quad +1\quad \frac{f_{NMB}e^{-i\phi}}{2}\frac{k_\perp m_B(1-y)}{y\sqrt{ym_Nm_B}}, \tag{A24}$$

$$\frac{1}{2}\to-\frac{3}{2},\quad 0\quad 0, \tag{A25}$$

$$\frac{1}{2}\to-\frac{3}{2},\quad -1\quad 0. \tag{A26}$$

In the above equations we have used the notation $1/2\to\lambda,\lambda'$, where λ and λ' are the helicities of the baryon and meson, respectively. y is the longitudinal momentum

fraction of the baryon and ϕ is the angle between the baryon's transverse momentum and that of the nucleon. g_{NMB} and f_{NMB} are the coupling constants which we choose [12,32,102] as $g^2_{p\pi^0 p}/4\pi=13.6$, $g^2_{p\rho^0 p}/4\pi=0.84$, $g^2_{p\omega p}/4\pi=8.1$, $f^2_{p\pi^- \Delta^{++}}/4\pi=10.85\ \mathrm{GeV}^{-2}$, $f^2_{p\rho^- \Delta^{++}}/4\pi=34.7\ \mathrm{GeV}^{-2}$, $f^2_{p\rho^0 p}/4\pi=31.25\ \mathrm{GeV}^{-2}$, and $f^2_{p\omega p}/4\pi=0$. Other coupling constants are related to these ones through the quark model [32,102,103].

[1] J. D. Sullivan, Phys. Rev. D **5**, 1732 (1972).
[2] F. Zamani and D. Saranchak, Phys. Rev. C **63**, 065202 (2001).
[3] F. Zamani, Phys. Rev. C **58**, 3641 (1998).
[4] A. W. Thomas, Nucl. Phys. **A518**, 186 (1990).
[5] S. Kumano, Phys. Rev. D **41**, 195 (1990).
[6] A. W. Thomas and G. A. Miller, Phys. Rev. D **43**, 288 (1991).
[7] W. Y. P. Hwang, J. Speth, and G. E. Brown, Z. Phys. A **339**, 383 (1991).
[8] S. Kumano, Phys. Rev. D **43**, 59 (1991).
[9] S. Kumano, Phys. Rev. D **43**, 3067 (1991).
[10] S. Kumano and J. T. Londergan, Phys. Rev. D **44**, 717 (1991).
[11] W. Melnitchouk, A. W. Thomas, and A. I. Signal, Z. Phys. A **340**, 85 (1991).
[12] V. R. Zoller, Z. Phys. C **53**, 443 (1992).
[13] A. W. Schreiber, P. J. Mulders, A. I. Signal, and A. W. Thomas, Phys. Rev. D **45**, 3069 (1992).
[14] W. Y. P. Hwang and J. Speth, Phys. Rev. D **46**, 1198 (1992).
[15] A. W. Thomas and W. Melnitchouk, *New Frontiers in Nuclear Physics* (World Scientific, Singapore, 1993), p. 41.
[16] A. Szczurek and J. Speth, Nucl. Phys. **A555**, 249 (1993).
[17] A. Szczurek, J. Speth, and G. T. Garvey, Nucl. Phys. **A570**, 765 (1994).
[18] N. N. Nikolaev, A. Szczurek, J. Speth, and V. R. Zoller, Z. Phys. A **349**, 59 (1994).
[19] B. C. Pearce, J. Speth, and A. Szczurek, Phys. Rep. **242**, 193 (1994).
[20] A. Szczurek, M. Ericson, H. Holtmann, and J. Speth, Nucl. Phys. **A596**, 397 (1996).
[21] A. Szczurek, A. J. Buchmann, and A. Faessler, J. Phys. G **22**, 1741 (1996).
[22] S. J. Brodsky and Bo-Qiang Ma, Phys. Lett. B **381**, 371 (1996).
[23] W. Koepf, L. L. Frankfurt, and M. Strikman, Phys. Rev. D **53**, 2586 (1996).
[24] F. M. Steffens and A. W. Thomas, Phys. Rev. C **55**, 900 (1997).
[25] S. D. Bass and D. Schutte, Z. Phys. A **357**, 85 (1997).
[26] S. Kumano, Phys. Rep. **303**, 183 (1998).
[27] F. S. Navarra, M. Nielsen, and S. Paiva, Phys. Rev. D **56**, 3041 (1997).
[28] S. Paiva, M. Neilson, F. S. Navarra, F. O. Duraes, and L. L. Barz, Mod. Phys. Lett. A **13**, 2715 (1998).
[29] V. R. Zoller, Mod. Phys. Lett. A **8**, 1113 (1993).
[30] F. M. Steffens, H. Holtmann, and A. W. Thomas, Phys. Lett. B **358**, 139 (1995).
[31] W. Melnitchouk and A. W. Thomas, Z. Phys. A **353**, 311 (1995).
[32] H. Holtmann, A. Szczurek, and J. Speth, Nucl. Phys. **A596**, 631 (1996).
[33] J. Speth and A. W. Thomas, Adv. Nucl. Phys. **24**, 83 (1997).
[34] K. G. Borekov, A. B. Kaidalov, Y. B. Dong, K. Shimizu, A. Faessler, and A. J. Buchmann, J. Phys. G **25**, 1115 (1999).
[35] S. Kumano and M. Miyama, Phys. Rev. D **65**, 034012 (2002).
[36] J. Ashman *et al.*, Phys. Lett. B **206**, 364 (1988).
[37] J. Ashman *et al.*, Phys. Lett. B **328**, 1 (1989).
[38] B. Adeva *et al.*, Phys. Lett. B **302**, 533 (1993).
[39] D. Adams *et al.*, Phys. Lett. B **329**, 399 (1994).
[40] D. Adams *et al.*, Phys. Lett. B **357**, 533 (1995).
[41] D Adams *et al.*, Phys. Lett. B **396**, 338 (1997).
[42] D. Adams *et al.*, Phys. Rev. D **56**, 5330 (1997).
[43] B. Adeva *et al.*, Phys. Lett. B **412**, 414 (1997).
[44] B. Adeva *et al.*, Phys. Rev. D **58**, 112001 (1998).
[45] B. Adeva *et al.*, Phys. Rev. D **60**, 072004 (1999).
[46] J. Le Goff *et al.*, Phys. Lett. A **666**, 296 (2000).
[47] P. L. Anthony *et al.*, Phys. Rev. Lett. **71**, 959 (1993).
[48] P. L. Anthony *et al.*, Phys. Rev. D **54**, 6620 (1996).
[49] K. Abe *et al.*, Phys. Rev. Lett. **74**, 346 (1995).
[50] K. Abe *et al.*, Phys. Rev. Lett. **75**, 25 (1995).
[51] K. Abe *et al.*, Phys. Lett. B **364**, 61 (1995).
[52] K. Abe *et al.*, Phys. Rev. Lett. **79**, 26 (1997).
[53] K. Abe *et al.*, Phys. Rev. D **58**, 112003 (1998).
[54] P. L. Anthony *et al.*, Phys. Lett. B **463**, 339 (1999).
[55] O. Rondon, Nucl. Phys. **A663**, 293 (1997).
[56] P. L. Anthony *et al.*, Phys. Lett. B **493**, 19 (2000).
[57] K. Ackerstaff *et al.*, Phys. Lett. B **404**, 383 (1997).
[58] A. Airapetian *et al.*, Phys. Lett. B **442**, 484 (1998).
[59] A. Simon *et al.*, Nucl. Phys. B, Proc. Suppl. **86A**, 112 (2000).
[60] A. Brull *et al.*, Nucl. Phys. **A663**, 2000 (2000).
[61] J. D. Bjorken, Phys. Rev. **148**, 1467 (1966).
[62] J. D. Bjorken, Phys. Rev. D **1**, 1376 (1970).
[63] J. Ellis and R. Jaffe, Phys. Rev. D **9**, 1444 (1974).
[64] G. Altarelli and G. G. Ross, Phys. Lett. B **212**, 391 (1988).
[65] R. D. Carlitz, J. C. Collins, and A. H. Mueller, Phys. Lett. B **214**, 299 (1988).
[66] A. V. Efremov, J. Soffer, and O. V. Teryaev, Nucl. Phys. **B246**, 97 (1990).
[67] G. T. Bodwin and J. Qiu, Phys. Rev. D **41**, 2755 (1990).
[68] S. D. Bass and A. W. Thomas, J. Phys. G **19**, 639 (1993).
[69] H. Y. Cheng, Chin. J. Phys. (Taipei) **38**, 753 (2000).
[70] J. Ellis and M. Karliner, hep-ph/9601280.
[71] R. L. Jaffe and A. Manohar, Nucl. Phys. **B337**, 509 (1990).
[72] M. Anselmino, A. Efremov, and E. Leader, Phys. Rep. **261**, 1 (1995).
[73] V. U. Stiegler, Phys. Rep. **277**, 1 (1996).
[74] I. Hinchliffe and A. Kwiatkowski, Annu. Rev. Nucl. Part. Sci. **46**, 609 (1996).
[75] G. P. Ramsey, Prog. Part. Nucl. Phys. **39**, 599 (1997).
[76] L. F. Li and T. P. Cheng, hep-ph/9709293.
[77] G. Altarelli, R. D. Ball, S. Forte, and G. Ridolfi, Acta Phys. Pol. B **29**, 1145 (1998).

[78] M. C. Vetterli, hep-ph/9812420.
[79] J. Kodaira and K. Tanaka, Prog. Theor. Phys. **101**, 191 (1999).
[80] B. Lampe and E. Reya, Phys. Rep. **332**, 1 (2000).
[81] P. A. M. Dirac, Rev. Mod. Phys. **21**, 392 (1949).
[82] H. Leutwyler and J. Stern, Ann. Phys. (N.Y.) **112**, 94 (1978).
[83] M. G. Fuda, Ann. Phys. (N.Y.) **197**, 265 (1990).
[84] M. G. Fuda, Ann. Phys. (N.Y.) **231**, 1 (1994).
[85] M. Burkardt, Adv. Nucl. Phys. **23**, 1 (1996).
[86] F. Schlumpf, Ph.D. thesis, University of Zurich, 1992.
[87] F. Schlumpf, Phys. Rev. D **47**, 4114 (1993).
[88] V. B. Berestetskii and M. V. Terent'ev, Sov. J. Nucl. Phys. **24**, 547 (1976).
[89] V. B. Berestetskii and M. V. Terent'ev, Sov. J. Nucl. Phys. **25**, 347 (1977).
[90] F. E. Close, Phys. Lett. **43B**, 422 (1973).
[91] A. De Rujula, H. Georgi, and S. L. Glashow, Phys. Rev. D **12**, 147 (1970).
[92] H. J. Melosh, Phys. Rev. D **9**, 1095 (1974).
[93] Z. Dziembowski, C. J. Martoff, and P. Zyla, Phys. Rev. D **50**, 5613 (1994).
[94] C. M. Shakin and Wei-Dong Sun, Phys. Rev. C **53**, 3152 (1996).
[95] H. M. Choi, Ph.D. thesis, North Carolina State University, 1999.
[96] V. N. Gribov and L. N. Lipatov, Sov. J. Nucl. Phys. **15**, 438 (1972).
[97] G. Altarelli and G. Parisi, Nucl. Phys. **B126**, 298 (1977).
[98] Yu. L. Dokshitzer, Sov. Phys. JETP **46**, 641 (1977).
[99] S. Kumano and J. T. Londergan, Comput. Phys. Commun. **69**, 373 (1992).
[100] R. Kobayashi, M. Konuma, and S. Kumano, Comput. Phys. Commun. **86**, 264 (1995).
[101] Y. Goto *et al.*, Phys. Rev. D **62**, 034017 (2000).
[102] B. Holzenkamp, K. Holinde, and J. Speth, Nucl. Phys. **A500**, 485 (1989).
[103] G. E. Brown and W. Weise, Phys. Rep., Phys. Lett. **22**, 281 (1975).
[104] S. J. Brodsky and F. Schlumpf, Phys. Lett. B **329**, 111 (1994).